

PREDICTING IN VIVO RNA SECONDARY STRUCTURE

by

Jiexin Gao

A thesis proposal submitted in conformity with the requirements
for the degree of Doctor of Philosophy
Graduate Department of Electrical Engineering
University of Toronto

© Copyright 2019 by Jiexin Gao

Abstract

Predicting in vivo RNA Secondary Structure

Jiexin Gao

Doctor of Philosophy

Graduate Department of Electrical Engineering

University of Toronto

2019

Contents

1	Introduction	1
1.1	RNA secondary structure	1
1.2	High throughput probing of RNS secondary structure	1
1.3	Deep neural network	1
2	Yeast Model	2
2.1	Training Dataset	2
2.2	Deep neural network	2
2.3	Training	4
2.4	Performance	4
2.4.1	Cross-validation performance on training dataset	4
2.4.2	Ribosomal RNA	4
2.4.3	Noncoding RNAs	5
2.5	Future Work	5
3	Mouse Model	8
4	Human Model	9
5	Conclusion and future work	10
	Bibliography	10

Chapter 1

Introduction

1.1 RNA secondary structure

1.2 High throughput probing of RNS secondary structure

1.3 Deep neural network

Chapter 2

Yeast Model

2.1 Training Dataset

To model in vivo RNA secondary structure, we compiled training data from [2]. In this study, yeast strain was treated with dimethyl sulphate (DMS), which reacts with unpaired adenine and cytosine bases. The pool of modified RNAs were fragmented and sequenced. Since DMS modification blocks reverse transcription, number of reads (TODO stops?) at each position is indicative of relative accessibility of that site.

Raw count data was downloaded from GSE45803 (`GSE45803_Feb13_VivoAllextra_1_15_PLUS.wig.gz` and `GSE45803_Feb13_VivoAllextra_1_15_Minus.wig.gz`). The authors aligned 25nt of each read to a non-redundant set of RefSeq transcripts, where each gene is represented by its longest protein-coding transcript. Only uniquely mapped reads with less than 2 mismatches were retained, and the authors further filtered out aligned reads whose RT stop is not A/C. The count at each position represents the combined number of RT stops at that site, across 4 biological replicates.

To construct training dataset, *Saccharomyces cerevisiae* assembly R61 (secCer2) RefSeq gene annotation was used to extract mRNA sequences. For each transcript, we first extract the raw read count for all adenine (A) and cytosine (C) bases (A/C positions with no RT stop coverage were set to a count of 0), and applied 90% Winsorization to remove outliers. Specifically, for each non-overlapping window of 100 A/C bases, values above the 95% percentile was set to the 95% percentile, and values below the 5% percentile was set to the 5% percentile. Then, all values within this window were divided by the max, to obtain values between 0 and 1.

2.2 Deep neural network

We construct a deep neural network to predict reactivity at single base resolution from RNA sequence context. We use an architecture similar to DenseNet[1], in which we've removed the pooling layers, to maintain the spatial resolution throughout the depth of the neural network.

As shown in Fig2.1, to make inference on a stretch of RNA sequence of length L , we need to pad the sequence with w bases on each side. (TODO explanation + how to calculate w) Input consists of the one-hot encoded, padded sequence, where A, C, G, U bases are encoded as $[1, 0, 0, 0]$, $[0, 1, 0, 0]$, $[0, 0, 1, 0]$, $[0, 0, 0, 1]$, respectively. The encoded input is then passed through multiple dense blocks, where each block consists

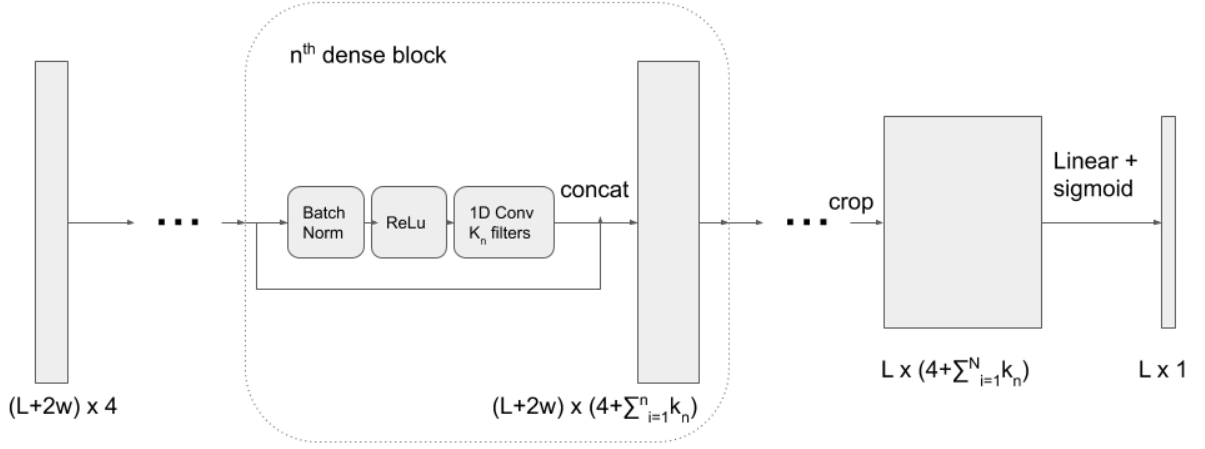


Figure 2.1: Densely connected neural network used for the yeast model

of four components:

1. Batch Normalization
2. ReLu nonlinear activation
3. 1D Convolution
4. Concatenation of the block input to the output of convolution

Block number	Number of filters	Filter width	Dilation rate
1	128	16	1
2	128	16	2
3	256	16	4
4	256	16	8
5	512	16	16

Table 2.1: Dense block parameters

We use 5 dense blocks in this work. The parameter of each layer is as shown in Table2.1. Densely connected block has the advantage that each block receives input from all preceding blocks, and passes its output to all successive blocks. The output of the last dense block essentially represents the features learnt from input at multiple resolutions.

The final dense block output is then cropped to account for the input padding, and then passed through a fully connected layer with sigmoid activation, along the feature dimension.

2.3 Training

Fold number	Chromosomes
1	chrM, chrVIII, chrII, chrXV
2	chrI, chrV, chrXIII, chrIV
3	chrVI, chrXI, chrXVI
4	chrIII, chrX, chrXII
5	chrIX, chrXIV, chrVII

Table 2.2: Chromosomes used for each fold

We use 5-fold cross validation, where the folds are split by chromosomes, as shown in Table 2.2.

Normalized data points (between 0 and 1) are used as soft targets without being converted to binary labels, and models were trained using a masked cross-entropy loss, as described below.

Due to the nature of DMS modification, G/T bases has no coverage, thus should be excluded from the calculation of the loss and the gradient. This is achieved by first computing the per position cross-entropy loss between the prediction and the target, then multiply it with a binary mask with the same shape as the target array. Positions with G/T bases are being set to 0 in the mask, while positions with A/C bases are 1. The masked loss are then summed over positions, and minibatch dimension, to calculate the loss for the current minibatch and the gradient for back propagation.

Models were trained using fixed sequence length of 50 (before padding, sequence length at inference time can be variable), minibatch size of 10, Adam optimizer with learning rate 0.0001 and momentum 0.9. To prevent the models from overfitting, L1 and L2 regularizers with weight 0.000001 was added to the loss, and training is stopped if validation loss hasn't improved over the last 10 epochs.

We trained 5 models, each using one of the folds as validation data, and the rest as training data.

2.4 Performance

2.4.1 Cross-validation performance on training dataset

We first evaluate the model performance on training dataset. For each transcript, we used the model that wasn't trained on its chromosome to make prediction for all A/C bases. We computed the Spearman correlation between the prediction and the target for each transcript. Fig 2.2 shows the distribution of Spearman correlation across all transcripts.

2.4.2 Ribosomal RNA

Next we used our model to predict the reactivity for all A/C bases in yeast 18S and 15S ribosomal RNAs, both were never seen by the model (neither in the training nor validation set).

Raw read count data for 18S and 15S was downloaded from GSE45803, and was processed similarly to the training dataset, since the experimental protocol was identical.

Correlation between prediction and the normalized read count is shown in Fig2.3 and Fig2.4, where each data point is one A/C base in the corresponding transcript. In comparison, RNAfold (window size 50 and span 50) achieves a correlation of 0.3217 and 0.4529 for 18S and 15S, respectively.

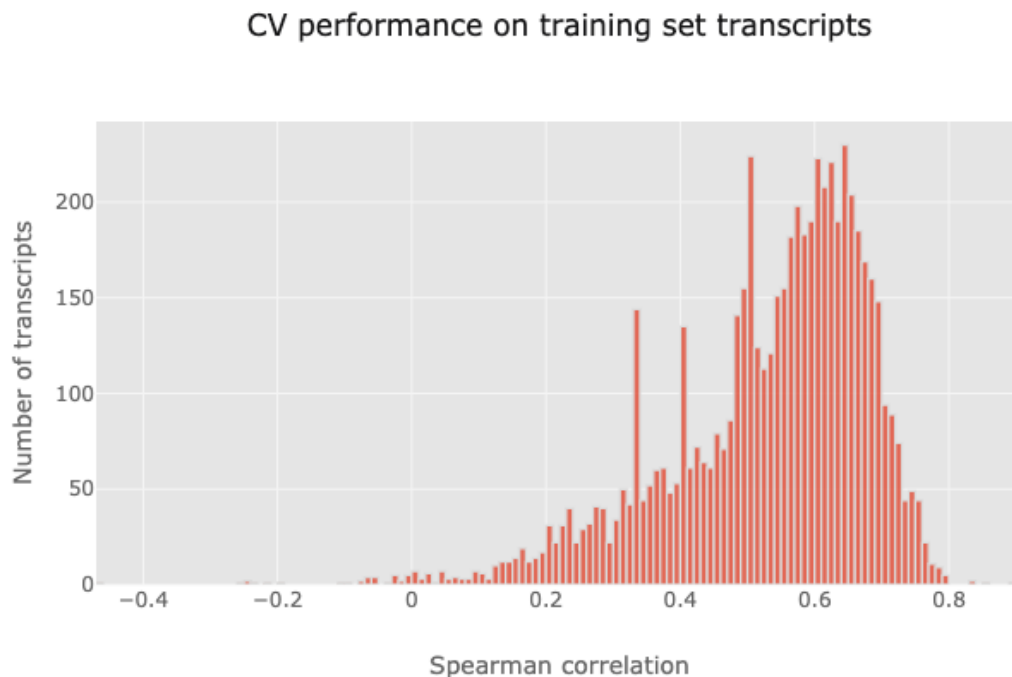


Figure 2.2: Densely connected neural network used for the yeast model

2.4.3 Noncoding RNAs

To evaluate whether the model generalizes to noncoding transcripts and different experimental protocol, we processed yeast data from the ModSeq paper[?], where yeast was treated with DMS or no-DMS (as control), and the authors identified positions that are significantly modified between treated and control, in selected noncoding and rRNA transcripts.

For each transcript, we use our models to predict on all A/C positions, and computed the au-ROC on how well the prediction distinguish the significantly modified bases from the rest. We also compare the performance of our model to that of RNAfold, as shown in Fig2.5.

2.5 Future Work

- Improve training and generalization performance, by making use of the raw sequencing data, and biological replicates. In addition to counts of RT stops, read coverage at each position can be used to infer the confidence of calling that position paired/unpaired. Transcript can be reweighted during training, according to the agreement between different biological reps.
- Multi-resolution learning.

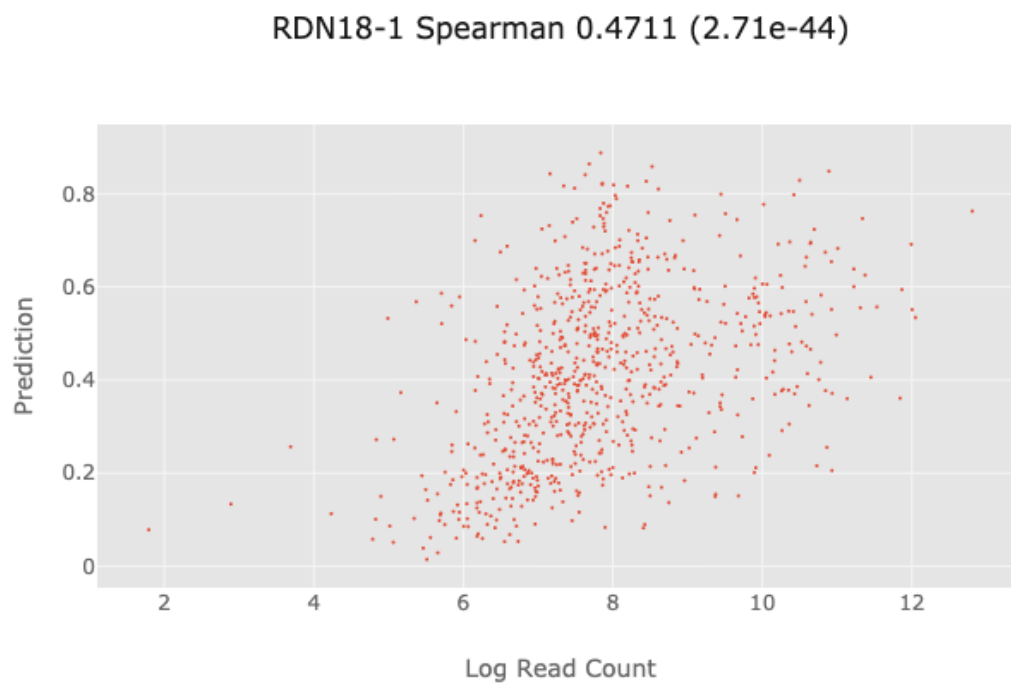


Figure 2.3: Densely connected neural network used for the yeast model

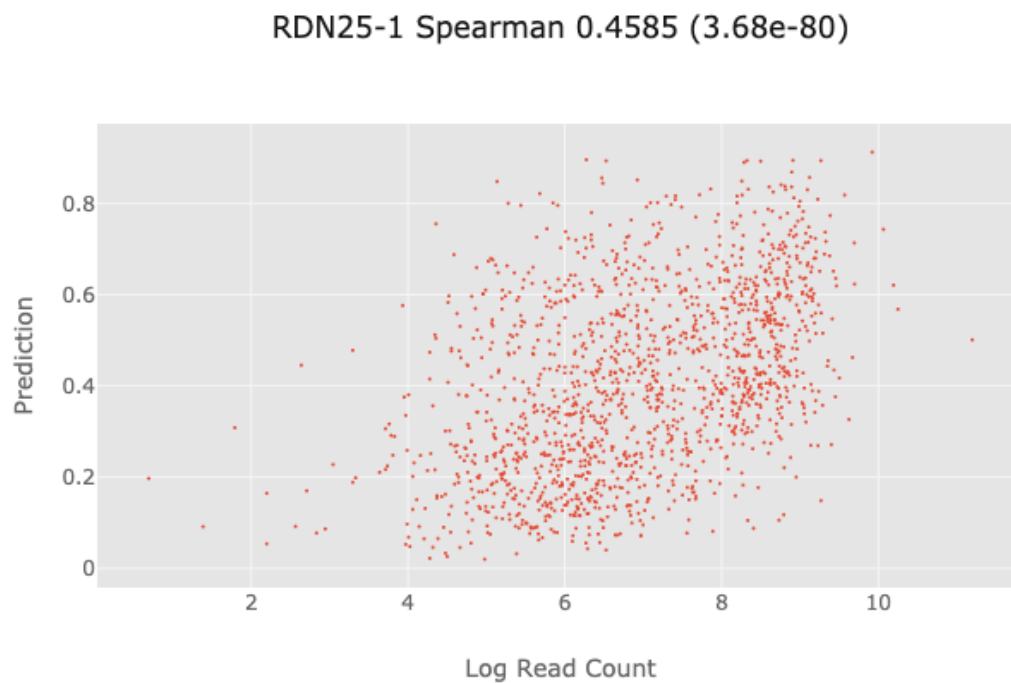


Figure 2.4: Densely connected neural network used for the yeast model

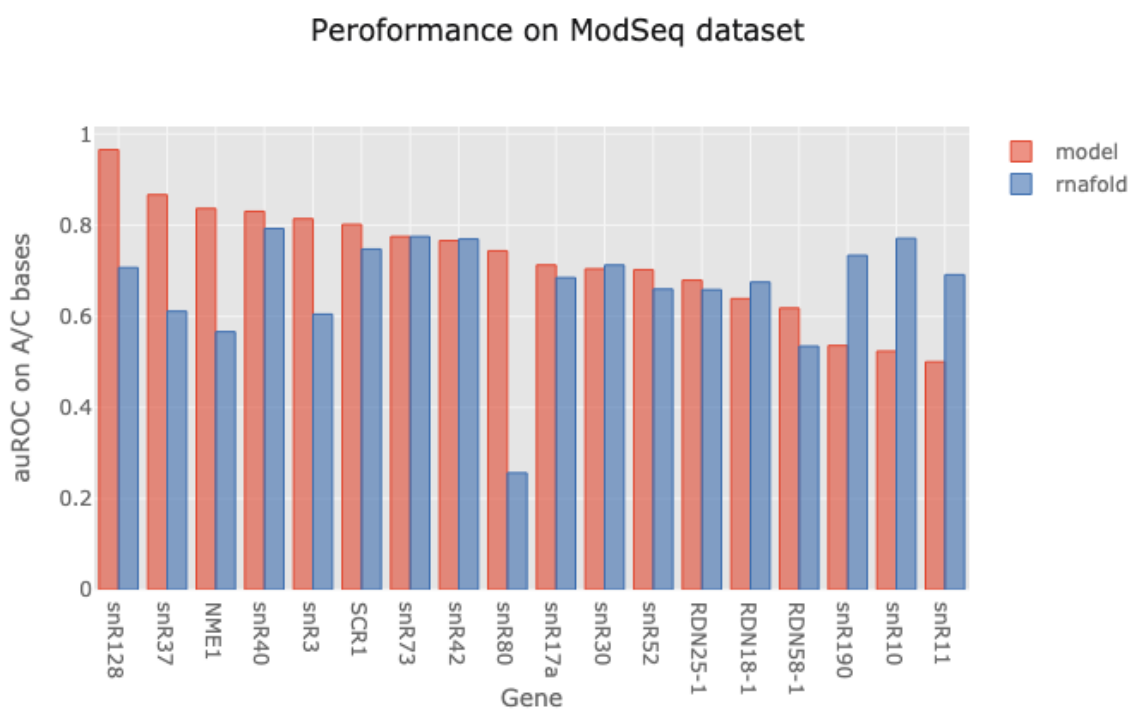


Figure 2.5: Densely connected neural network used for the yeast model

Chapter 3

Mouse Model

Chapter 4

Human Model

Chapter 5

Conclusion and future work

one dataset that has multiple mods per sequence, so we can reconstruct collection of structures
joint learning of accessibility and other data, e.g. chip-seq peaks

Bibliography

- [1] Gao Huang, Zhuang Liu, Laurens Van Der Maaten, and Kilian Q Weinberger. Densely connected convolutional networks. In *Proceedings of the IEEE conference on computer vision and pattern recognition*, pages 4700–4708, 2017.
- [2] Silvi Rouskin, Meghan Zubradt, Stefan Washietl, Manolis Kellis, and Jonathan S Weissman. Genome-wide probing of rna structure reveals active unfolding of mrna structures in vivo. *Nature*, 505(7485):701, 2014.